Adsorption and Decomposition Pathways of Vinyl Phosphonic and Ethanoic Acids on the Al(111) Surface: a Density Functional Analysis

ARTICLE *in* THE JOURNAL OF PHYSICAL CHEMISTRY C · APRIL 2007

Impact Factor: 4.77 · DOI: 10.1021/jp0667487

1 AUTHOR:

Jun Zhong
Arizona State University
8 PUBLICATIONS **62** CITATIONS

SEE PROFILE

Adsorption and Decomposition Pathways of Vinyl Phosphonic and Ethanoic Acids on the Al(111) Surface: a Density Functional Analysis

Jun Zhong

School of Materials, Arizona State University, Tempe, Arizona 85287-8706

James B. Adams*

School of Materials, Arizona State University, Tempe, Arizona 85287-8706

Received: October 13, 2006; In Final Form: February 26, 2007

Density functional theory is employed to investigate optimal adsorption geometries and binding energies of vinyl phosphonic and ethanoic acids on the Al(111) surface. Tribridged, bi-bridged, and unidentate coordinations for adsorbates are examined to determine optimal binding sites on the surface. An analysis of charge density of states of oxygen involved in reacting with aluminum ions reveals changes in atomic bonding. For these acid molecules, the favorable decomposition pathways lead to fragments of vinyl and alkyl chains bonding to the Al(111) surface with phosphorus and carbon ions. The final optimal decomposition geometries and binding energies for various decomposition stages are also discussed.

1. Introduction

Lubricant formulations used to control friction and wear in metallic forming processes typically contain mixtures of additive molecules in the base oil. Common lubricant additives for aluminum rolling processes are fatty acid molecules such as vinyl phosphonic and ethanoic acids which consist of cationic anchors of electron rich functional groups like oxygen-rich bases. These molecules are thought to interact with the aluminum surface to form protective thin films that are several molecular layers thick. The functional groups on these molecules can be decomposed on the "islands of nascent aluminum" formed during aluminum rolling. The adsorption/decomposition products will contribute to boundary thin-film lubrication of plastically deforming interfaces.

To understand the adhesion mechanism of these boundary-layer lubricants, vinyl phosphonic acid (VPA), $H_3C_2P(O)(OH)_2$, was chosen as one of representative organo-phosphorus acids.[1,2] Figure 1a shows one illustration of this molecular structure. This molecule contains a phosphorus atom serving as a cationic anchor for two electron-rich functional groups; that is, it consists of a tripodal "oxygen-rich" base plus a vinyl hydrocarbon tail. Inelastic tunneling spectroscopy (IETS) of VPA adsorption on the aluminum oxide surface implied that the vinyl group on VPA did not participate in bonding to the oxide surface.[3] Hence, this reaction resulted in a tridentate coordination with a tripodal "oxygen-rich" base; that is, the reacted species served as a molecular cap that may inhibit the migration of corrosive species into the oxide surface but may leave the vinyl group accessible to react with lubricants. In addition, tridentate coordination was not unique to VPA since it had been noted for other phosphonic acids.[4] Another organic hydrocarboxylic acid, ethanoic acid (EA), $H_3C_2(O)(OH)$, with an alkyl chain plus a bipodal "oxygen-rich (OOH)" base, shown in Figure 1b, was used to study interaction with the Al(111) surface to obtain a fundamental understanding of reactivity of aluminum surfaces toward this class of aliphatic acid molecule. One study used electron energy loss spectroscopy (EELS) to investigate EA adsorption on the Al(111) surface starting at a very low temperature (120 K).[5,6] It found that the symmetrically bi-bridged bonding orientation of a dissociated EA piece was more likely than other bonding configurations in thin-film on the surface. Both of the above-mentioned studies found that the "oxygen-rich" bases on these acid molecules bound to and oxidized the aluminum surface, and the residual molecular fragments formed thin-film inhibitors on the surface.

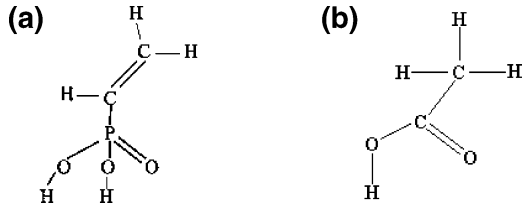

Figure 1. Two acid molecules: (a) VPA molecule and (b) EA molecule.

Methods in density functional theory such as local density approximation/generalized gradient approximation (DFT−LDA/GGA) have been used to investigate adsorption/decomposition of different molecular additives on metal surfaces. For example, Scheffler et al. analyzed various adsorption sites on aluminum surfaces for alkali atoms. They found that alkali atoms on the close-packed Al(111) surface can adsorb at on-top sites or substitutional ones where alkali atoms replaced atoms at the substrate surface.[7] Zhou et al. calculated adsorption energies of some small organic molecules (methanol, ethylene, ketone, and dimethyl ether) on a clean Al(111) surface. They found that the calculated adsorption energies were in good agreement with experimental values; that is, the adsorption energy of these organic compounds was found to order in the following way: methanol > ketone > dimethyl ether > ethylene.[8] Jiang et al. calculated adsorption energies of the benzotriazole (BTAH or

* Corresponding author.

10.1021/jp0667487 CCC: $37.00
Published on Web 05/01/2007

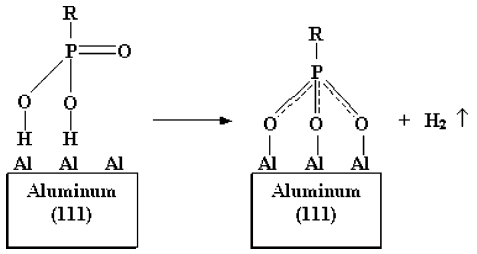

Figure 2. Proposed reaction pathway for VPA adsorption on the Al-(111) surface in tribridged coordination.

$C_6N_3H_5$) molecule on a clean Cu(111) surface[9] and Cu_2O(111) surface.[10] They found that BTAH could be physisorbed or weakly chemisorbed on these surfaces through evolution of nitrogen sp^2 lone pairs on BTAH. Following observations of IETS, Hector et al. investigated reaction enthalpies of VPA on an idealized α-Al_2O_3(0001) surface in several adsorbing geometries: tridentate, bidentate, and unidentate coordinations. They concluded that each VPA bound to an alumina slab as a consequence of acid−base reactions with the oxide surface. These reactions occurred at deprotonated hydroxyl (OH) and phosphoryl oxygen groups on VPA and hydroxyl (OH) groups on the alumina surface.[11] The most favorable adsorption pathway was tridentate coordination, while unidentate coordination was the least favorable. The above-mentioned research usually focused on the preliminary adsorption step of adsorbate molecules on metal surfaces but did not consider further molecular decompositions on these surfaces.

In our present article, we carry out serial DFT calculations to analyze how two commonly used boundary thin-film lubricants, VPA and EA, bind to the Al(111) surface. Since nascent islands of bare aluminum will be formed during rolling and forming processes on the surface, it is very important that boundary thin-film lubricants bind to the highly reactive clean metal surface and prevent it from bonding to rolling tool surfaces, which would reduce severe adhesion.

A proposed diagram of one adsorption pathway for the reaction of VPA on the Al(111) surface is shown in Figure 2. In this figure, the chemisorbed VPA is assumed to stand on the Al(111) surface with its three symmetrical phosphorus−oxygen−aluminum (P−O−Al) bonds in a tribridged coordination. This reaction leads to the liberation of H ions from OH groups on VPA, resulting in the formation of H_2 molecules (H_2O if O_2 is present or both H_2 and H_2O). Note that "R" represents a vinyl functional group (H_2CCH), and the dashed lines indicate a resonant-stabilized conformation in which phosphorus atom is isotetrahedrally coordinated.[12] This model is the most stable adsorption configuration on the Al(111) surface. In the case of EA adsorption on such a surface, similar reaction products can be seen in which an EA fragment (acetate) is in a symmetrically bi-bridged coordination on the Al(111) surface, with liberation of H ions from EA to form free gaseous H_2 molecules. Furthermore, similar adsorption geometries like above two should be applicable to a wide variety of similar lubricants.

In addition, we examine states along likely decomposition pathways of EA and VPA on the Al(111) surface. Total binding energies are calculated for each step of the dissociation process for both EA and VPA adsorbates on the Al(111) surface.

2. Computational Methodology

Our calculations were based on DFT[13−15] using Vienna Ab-Initio Simulation Package (VASP): All calculations were performed using Vanderbilt-type ultra-soft pseudopotentials (USP)[16] or projector-augmented wave (PAW) pseudopotentials.[17] The GGA created by Perdew and co-workers[18,19] was employed for evaluation of exchange-correlation energy. This methodology was similar to our previous studies of optimal adsorption geometries for VPA on the α-Al_2O_3(0001) surface.[11]

TABLE 1: Bulk Properties of Aluminum by Fitting to the Murnaghan Equation

method	lattice constant a (Å)	cohesive energy E_{coh} (eV)	bulk modulus B_0 (eV/Å^3)
VASP-US-GGA	4.049	−3.690	0.4244
VASP-PAW-GGA	4.053	−3.694	0.4307
LDA [ref 33]	3.971	−4.090	0.4774
experiment	4.030 [ref 36]	−3.36 [ref 21]	0.4956 [ref 37]

TABLE 2: Bond Energies on VPA and EA (unit: eV)

VPA		EA	
P═O	P−O	C═O	C−O
5.64	3.68	8.28	3.71

Prior to studies of VPA and EA adsorptions on the Al(111) surface, we calculated the lattice constant, bulk modulus, and cohesive energy for a pure aluminum bulk by fitting data of energy versus volume to the Murnaghan equation.[20] A regular Monkhorst−Pack grid of 17 × 17 × 17 was chosen as the best k-point sampling. The total energy was converged within 1∼2 meV. The LDA and GGA calculated bulk properties of pure aluminum are listed in Table 1. Comparing to former calculations in our research group,[33] our results are in reasonable agreement with experimental data for the lattice constant a and bulk modulus B_0 but are slightly high for cohesive energy E_{coh}.

Comparing PAW-GGA to US-GGA, we found the PAW-GGA to be more efficient than the US-GGA; that is, the former cost less computational time and was slightly more reliable than the latter. For this reason, the PAW-GGA pseudopotential was used for all of the following Al slab calculations. In addition, tests of plane wave cutoff and k-point sampling[22] for systems were conducted to determine an optimal setting of these quantities for all ensuing calculations.[23]

Calculations of acid adsorption on the Al(111) surface were conducted in a super-cell geometry with a periodic four-layer 3 × 3 units Al(111) slab (16 ions per layer) in XY directions. We adopted a plane-wave cutoff energy of 400 eV, which was primarily required by the "hardest" ions (C and O). A Monkhorst−Pack grid of a 5 × 5 × 1 k-point sampling was selected for this orthogonal super-cell with three definitely orientated vectors: $a[110] = 11.31$ Å in the X axis, $b[11\bar{2}] = 9.90$ Å in the Y axis, and $c[111] = 26.00$ Å in the Z axis, along with a vacuum distance of 10.00 Å in c direction and with one bottom layer of the aluminum slab fixed in the super-cell. The optimal atomic geometry was achieved by minimizing Hellman−Feyman forces using a conjugate gradient and quasinewton algorithms, until the total force on each ion had reduced to 0.05 eV/Å or less.[24]

3. Conformations of VPA and EA Molecules

3.1. Structure of the VPA Molecule. Figure 3 shows a side view of one VPA molecular structure along with isosurfaces of charge density expressed with an electron (e^-) localization function (ELF) which represents the probability of finding a second e^- with the same spin in the neighboring region of the reference e^- within [0, 1]. In other words, a high ELF value means that the reference e^- is highly localized.[23−25] By definition, high ELF values are typically associated with covalent bonds, e^- lone pairs, or inert cores.[9] In Figure 3b, ELF

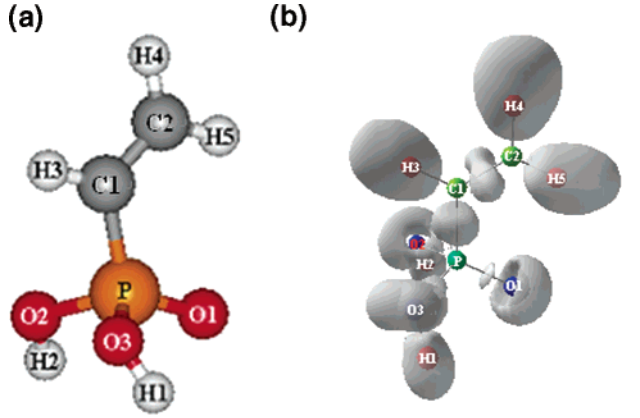

Figure 3. Side view of VPA conformation: (a) vinyl group and tripodal-based P−O bonds on VPA and (b) isosurfaces of charge density at ELF = 0.81 on VPA.

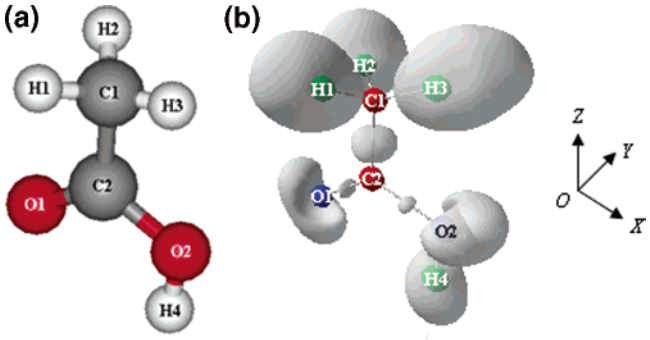

Figure 4. Side view of EA conformation: (a) methyl group and bipodal-based C−O bonds on EA and (b) isosurfaces of charge density at ELF = 0.67 on EA.

= 0.81 is chosen as the best visual difference of isosurfaces on each of the atomic bonds according to comments in ref 11.

VASP calculations for VPA indicate that two e^- lone pairs aggregate to O2 nearby (a circle-lunar lobe) because of its aniso-sp^3 hybrid bonding to H2 and P neighbors; the same is true for O3. However, O1 forms a weak double bond with P and has slightly more e^- lone pairs (a hemisphere lobe) than O2 and O3; see charge density of states in Figure 5a.

In Figure 3a, such a VPA conformation is the most favorably energetic with the vinyl group coplanar with the P═O1 double bond and is consistent with that predicted in ref 26.

3.2. Structure of the EA Molecule. Figure 4 shows a side view of one EA molecule, along with isosurfaces of charge density at ELF = 0.67, chosen to provide the best visual difference of isosurfaces on each atomic bond. VASP analyses for EA indicate that two e^- lone pairs aggregate to O2 nearby (a hemisphere lobe) because of its aniso-sp^3 hybrid bonding to H4 and C2 neighbors. However, a strong C2═O1 double bond results in lower charge density in e^- lone pairs around O1 (a semilunar lobe) than around O2; see charge density of states in Figure 5b.

Figure 5a,b shows distributions of charge density of states (DOS) for three O atoms on VPA and those for two O atoms on EA, respectively. In this figure, the E_{lumo} represents the energy level corresponding to the lowest unoccupied molecular orbital. Also, around the E_{lumo}, the DOS of O atoms represent their unoccupied states. From Figure 5, more DOS contributions above the E_{lumo} for O atoms on VPA than those on EA imply that VPA may be more reactive with the aluminum surface than EA through the O atoms.

4. Adsorption Sites on the Al(111) Surface for Adsorbates

Figure 6 shows three distinguishable adsorption sites in the top layer of the Al(111) surface. We refer to them as site-1, -2, and -3, respectively. Among these sites, site-1 (S-1) has corners at three Al ions, site-2 (S-2) has corners at three cave points (cross signs), and site-3 (S-3) has corners at three saddle points (ice-star signs). Through our experience, these sites are most likely for VPA and EA adsorptions on the Al(111) surface because they allow stronger bonding of the Al(111) surface to "oxygen-rich" bases on VPA and EA than other sites.

5. Analyses of VPA and EA Adsorption Configurations on the Al(111) Surface

To better understand the mechanism of VPA and EA adsorptions on the Al(111) surface, we carried out density functional calculations for the combined adsorbate/substrate system. The adsorption enthalpy (binding energy or binding strength), $\Delta H_{ads}^{(m)}$, is defined as the difference between the total energy of the combined adsorbate/substrate system and the total energy of the separated adsorbate and substrate, which is given by

$$\Delta H_{ads}^{(m)} = E(\text{adsorbate/substrate}) - [E(\text{adsorbate}) + E(\text{substrate})] \quad (5.1)$$

where the superscript (m) indicates reaction type. A negative value of $\Delta H_{ads}^{(m)}$ corresponds to a favorable reaction on the Al-(111) surface, while a positive one represents an unlikely reaction on the surface.

Generally, one VPA molecule has three different conformational (tripodal, bipodal, and unipodal) bases while one EA molecule has two different conformational (bipodal and unipodal) bases, which are involved in the adsorption. Here, we will investigate adsorption at site-1, -2, and -3. For each possible conformation, a total of nine geometries on VPA and six geometries on EA are adopted.

5.1. Initial Stage of Adsorption. Figure 7 shows side views of two optimized VPA and EA geometries at S-1 on the Al-(111) surface at the initial stage of adsorption. For VPA at this stage, only the O1 atom weakly anchors to the surface, while the hydroxyl (OH) groups are not involved in adsorption. The whole VPA molecule stays in a unidentate coordination on the surface. The relevant reaction pathway is given by

$$\text{VPA} + \text{Al} \rightarrow H_3C_2(OH)_2P{\approx}O...\text{Al}, \quad \Delta H^{(5.2)}{}_{ads} = -0.72\ \text{eV} \quad (5.2)$$

involving a partial breaking of the P═O double bond to P≈O. Similarly, for EA at this stage, only the O1 atom anchors to the surface and the whole EA molecule stays in a unidentate coordination on the surface. The relevant reaction pathway is given by

$$\text{EA} + \text{Al} \rightarrow H_3C(OH)C{=}O...\text{Al}, \quad \Delta H^{(5.3)}{}_{ads} = -0.07\ \text{eV} \quad (5.3)$$

indicating Van de Waals' interaction.[9]

Table 2 lists some relevant bond energies on VPA and EA molecules,[34] which are involved in reactions with the Al(111) surface during the above-mentioned adsorptions.

Comparing eqs 5.2 and 5.3, we find the binding energy for VPA adsorption on the Al(111) surface to be much stronger

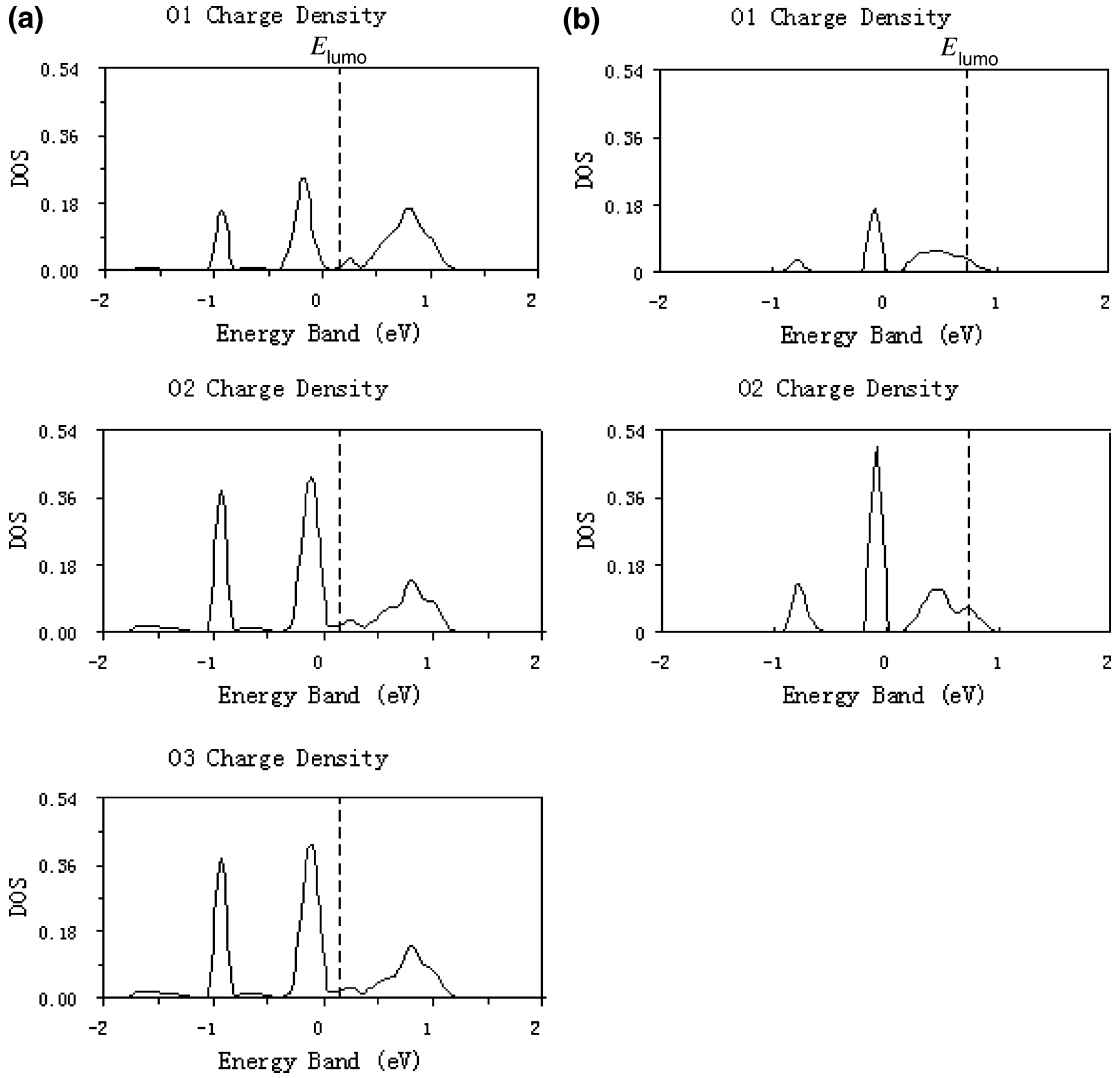

Figure 5. Charge density of states (DOS) for O atoms on VPA and EA molecules: (a) DOS for O atoms on VPA and (b) DOS for O atoms on EA.

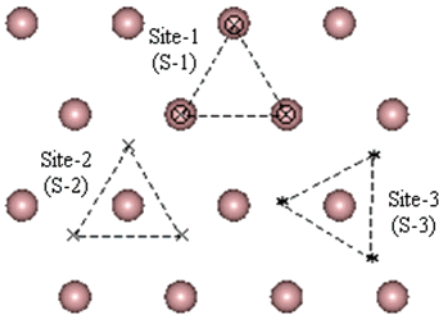

Figure 6. Three most favorable adsorption sites in the top layer of the Al(111) surface.

than that for EA adsorption on the surface. The reason is that the P═O double bond on VPA is relatively weak and likely broken (P═O → P—O, $\Delta E = 5.64 - 3.68 = 1.96$ eV) to cause a weak chemisorption, whereas the C═O double bond is too strong and does not appear to break, resulting in a weak physisorption (C═O → C—O, $\Delta E = 8.28 - 3.71 = 4.57$ eV).

Studies for VPA adsorptions at S-2 and S-3 on the Al(111) surface indicate that these adsorption sites are unstable. That is, VPA starting at S-2 or S-3 geometries always shifts to S-1 on the surface during energy minimization without any barriers. Similar results can be obtained for EA adsorption at S-2 and S-3 on the Al(111) surface. Therefore, S-1 is the most favorable site for these acid adsorptions/decompositions on the Al(111) surface. Because of this, we will only focus on the S-1 site for our investigations of VPA and EA adsorptions on the Al(111) surface.

5.2. Further Stages of Adsorption with the OH Group. In this section, we discuss further stages of VPA and EA adsorptions on the Al(111) surface involved in OH groups. Since OH groups are more active than others (e.g., null O groups), on such two acid molecules, they are more likely to first react with the surface to form strong Al—O bonds between adsorbates and adsorbents.[11,31] Therefore, after the initial stage of adsorption, VPA and EA should become deprotonated fragments at S-1 on the Al(111) surface, which are named vinyl phosphonate [$H_3C_2PO_3^{2-}$ and $H_3C_2PO_2(OH)^-$] and acetate [H_3CCOO^-], respectively. On the basis of experimental observations,[12,26] we assume the following: (1) Vinyl phosphonate may anchor to the Al(111) surface at S-1 in unidentate, bi-bridged, and tribridged coordinations by means of its "oxygen-rich" base. Similarly, acetate may anchor to the Al-(111) surface at S-1 through its "oxygen-rich" base in unidentate and bi-bridged coordinations. (2) For a convenient comparison of the binding energies between VPA and EA adsorptions on the surface, H ions liberated from these acid molecules through the condensing reaction either are assumed to be singly adsorbed on the surface or form gaseous H_2 molecules that leave the

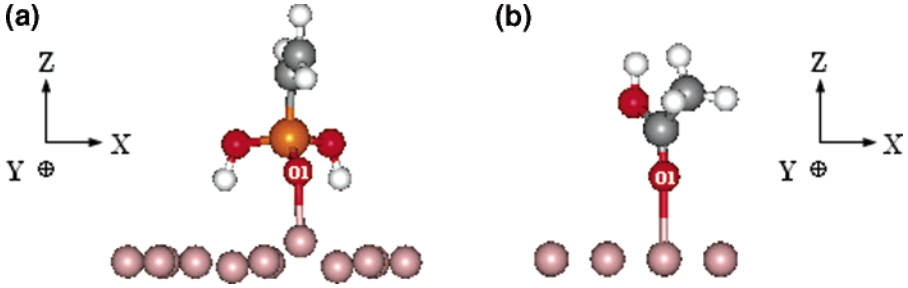

Figure 7. Side views of VPA and EA configurations on the Al(111) surface at the initial stage of adsorption: (a) VPA at S-1 on the surface and (b) EA at S-1 on the surface.

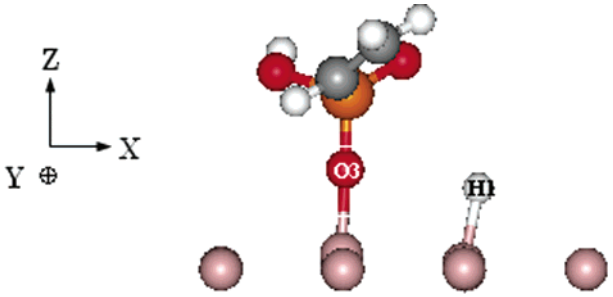

Figure 8. Side view of vinyl phosphonate adsorption in unidentate coordination plus one H ion adsorbed on the Al(111) surface.

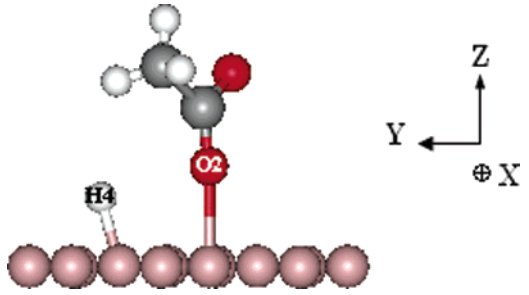

Figure 9. Side view of acetate adsorption in unidentate coordination plus one H ion adsorbed on the Al(111) surface.

surface. Furthermore, the adsorption of H ions on the surface also influences finally binding energies. (3) The vinyl chain on vinyl phosphonate and the alkyl chain on acetate will not be involved in adsorptions. Instead, they remain free to interact with other lubricants. Therefore, total adsorption geometries are analyzed as follows.

A. Unidentate Coordination for Adsorption. In this section, we consider how VPA anchors to the Al(111) surface at S-1 through an oxygen after one H ion is liberated from adsorbate. Figure 8 shows a side view of such adsorption in a unidentate coordination. The relevant reaction pathway is given by

$$\mathrm{VPA} + 2\mathrm{Al} \rightarrow \mathrm{H_3C_2(O)(OH)P{-}O...Al} + \mathrm{H...Al},$$
$$\Delta H^{(5.4a)}_{\mathrm{ads}} = -0.89\ \mathrm{eV} \quad (5.4a)$$

Comparing reactions in eqs 5.2 and 5.4a, we find that the reaction in eq 5.4a has a larger reaction enthalpy; that is, it is favorable for VPA to give up a H ion onto the surface, forming Al−H and Al−O single bonds while breaking its O−H single bond during adsorption.

Moreover, a VASP calculation indicates that the formation enthalpy for gaseous H_2 molecules through H atoms desorbed from a clean Al(111) surface: $\Delta H^* = -0.53$ eV, if ignoring zero point energy corrections. That is, the formation of gaseous H_2 molecules is favorable compared with adsorption of individual H ions on the surface. Thus, the continuous reaction for eq 5.4a followed by a H_2 formation could be described as

$$\mathrm{H_3C_2(O)(OH)P{-}O...Al} + \mathrm{H...Al} \rightarrow \mathrm{H_3C_2(O)(OH)P{-}O...Al} + \frac{1}{2}\mathrm{H_2}\uparrow,$$
$$\Delta H^{(5.4b)}_{\mathrm{ads}} = -0.26\ \mathrm{eV} \quad (5.4b)$$

Here, the formation enthalpy for a gaseous H_2 molecule through H atoms is obtained by VASP calculation: $\Delta H_{H_2} = -6.75$ eV. Regarding more comments, see ref 28. Similarly, H ions could react with O_2 or other spieces as well.

Figure 9 shows a side view of acetate adsorption on the Al(111) surface with its single C−O bond in unidentate coordination. In this figure, the H ion liberated from the OH group through the condensing reaction is also adsorbed on the surface. The relevant reaction pathway is given by

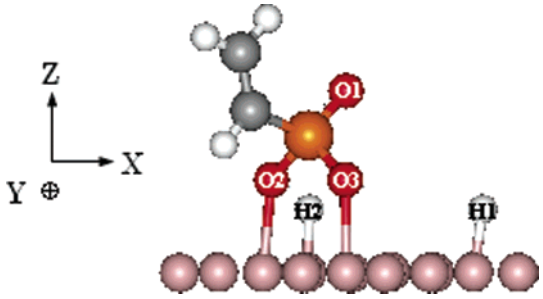

Figure 10. Side view of vinyl phosphonate adsorption in bi-bridged coordination plus two H ions adsorbed on the Al(111) surface.

$$\mathrm{EA} + 2\mathrm{Al} \rightarrow \mathrm{H_3C(O)C{-}O...Al} + \mathrm{H...Al},$$
$$\Delta H^{(5.5a)}_{\mathrm{ads}} = -0.51\ \mathrm{eV} \quad (5.5a)$$

Similar to the reaction in eq 5.4b, the next reaction pathway for eq 5.5a could be a formation of free gaseous H_2 molecules through two H atoms desorbed from the surface; that is,

$$\mathrm{H_3C(O)C{-}O...Al} + \mathrm{H...Al} \rightarrow \mathrm{H_3C(O)C{-}O...Al} + \frac{1}{2}\mathrm{H_2}\uparrow,$$
$$\Delta H^{(5.5b)}_{\mathrm{ads}} = -0.27\ \mathrm{eV} \quad (5.5b)$$

The result in eq 5.5b is very similar to that in eq 5.4b. Therefore, both reactions in eqs 5.4b and 5.5b are favorable; thus, the desorption of H ions from the Al(111) surface is more likely to occur.

B. Bi-bridged Coordination for the Adsorption. Subsequent to eq 5.4a in part A, the remaining P−OH group on vinyl phosphonate will anchor to the Al(111) surface at S-1, along with the liberation of a H ion from the adsorbing OH group. Figure 10 shows side views of such adsorption geometries; thus, the relevant reaction pathway is given by

$$\text{VPA} + 4\text{Al} \rightarrow H_3C_2(O)P-(2O)...2Al + 2H...2Al, \quad \Delta H^{(5.6a)}_{ads} = -1.32 \text{ eV} \quad (5.6a)$$

Consequently, the next reaction step for eq 5.6a could be a formation of a gaseous H_2 molecule through H atoms desorbed from the surface; the relevant reaction pathway is given by

$$H_3C_2(O)P-(2O)...2Al + 2H...2Al \rightarrow H_3C_2(O)P-(2O)...2Al + H_2\uparrow, \quad \Delta H^{(5.6b)}_{ads} = -0.51 \text{ eV} \quad (5.6b)$$

Obviously, the product in eq 5.6b is more favorable than that in eq 5.6a. Thus, it is favorable for H ions to desorb from the surface.

Similarly, following eq 5.5a in part A, EA can also bind to the surface in a bi-bridged fashion; see Figure 11. One H ion liberated from EA through the condensing reaction is adsorbed on the surface; the relevant reaction pathway is given by

$$\text{EA} + 3\text{Al} \rightarrow H_3CC-(2O)...2Al + H...Al, \quad \Delta H^{(5.7a)}_{ads} = -1.52 \text{ eV} \quad (5.7a)$$

Consequently, the next reaction step for eq 5.7a could be a formation of a freely gaseous H_2 molecule through two H atoms desorbed from the surface; the relevant reaction pathway is given by

$$H_3CC-(2O)...2Al + H...Al \rightarrow H_3CC-(2O)...2Al + \frac{1}{2}H_2\uparrow, \quad \Delta H^{(5.7b)}_{ads} = -0.26 \text{ eV} \quad (5.7b)$$

Obviously, the product in eq 5.7b is more favorable than that in eq 5.7a. The desorption of H ions from the surface is more likely to occur.

C. Tribridged Coordination for the Adsorption. In this section, following eq 5.6a in part B, the remaining P═O bond on vinyl phosphonate will be involved in the condensing reaction. Figure 12 shows a side view of VPA adsorption on the Al(111) surface in tribridged coordination. In this figure, two H ions liberated from VPA through the condensing reaction are adsorbed on the surface. The relevant reaction pathway is given by

$$\text{VPA} + 5\text{Al} \rightarrow H_3C_2P-(3O)...3Al + 2H...2Al, \quad \Delta H^{(5.8a)}_{ads} = -2.61 \text{ eV} \quad (5.8a)$$

Consequently, the next reaction step for eq 5.8a could be a formation of a gaseous H_2 molecule through two H atoms desorbed from the surface; the reaction pathway is given by

$$H_3C_2P-(3O)...3Al + 2H...2Al \rightarrow H_3C_2P-(3O)...3Al + H_2\uparrow, \quad \Delta H^{(5.8b)}_{ads} = -0.51 \text{ eV} \quad (5.8b)$$

Obviously, the product in eq 5.8b is more favorable than that in eq 5.8a. The desorption of H ions from the surface is more likely to occur.

In summary, assuming entropy contributions are negligible, for VPA, the most favorable reaction geometries on the Al(111) surface are in the following order:

tribridged coordination > bi-bridged coordination > unidentate coordination.

While for EA, the best reaction geometries on the Al(111) surface are in the order bi-bridged coordination > unidentate coordination.

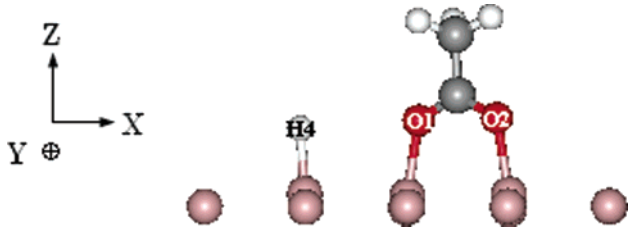

Figure 11. Side view of acetate adsorption in bi-bridged coordination plus one H ion adsorbed on the Al(111) surface.

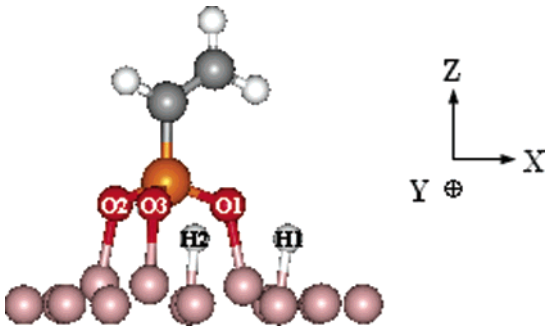

Figure 12. Side view of vinyl phosphonate adsorption in tribridged coordination plus two H ions adsorbed on the Al(111) surface.

Comparing these two adsorption types, in each of above corresponding adsorption geometries, we find that the relevant binding energy for VPA adsorption on the surface is always stronger than that for equivalent EA adsorption on the surface. The main reason should be highly reactive O—P═O functional groups, which will be discussed further in part D. In addition, H ion adsorptions also influence all of the above binding energies. However, our final calculations indicate that the formation of gaseous H_2 molecules through H atoms desorbed from the surface is favorable, although the desorbed H atoms may also react with other species.

D. DOS Analyses for Further Discussions. In this section, we discuss essential differences in the binding energies for VPA and EA adsorptions on the Al(111) surface by means of DOS analyses. Since, after adsorption, all of the P—O bonds reacting with the surface have very similar bond lengths, they should also have very similar bonding energies. The same is true for C—O bonds in EA. For a clear comparison, we analyze one of the unidentate adsorption geometries for both VPA and EA.

1. DOS Analyses. Figure 13 shows isosurfaces of charge density for vinyl phosphonate and acetate on the Al(111) surface in their unidentate coordinations, respectively. A value of ELF = 0.67 was used because it may provide the greatest visual difference in charge density on C—O and P—O bonds. Thus, in Figure 13b, a small lobe can be observed on the C2—O2 bond, while the P—O3 bond has no such character. This means that O2 on the C2—O2 bond is more covalent, while O3 on the P—O3 bond is more ionic. This is expected because P is less electronegative than C (2.1 vs 2.5).[35]

During adsorptions, the charge density for O3 on vinyl phosphonate in Figure 13a moves more toward the reacting Al ion in the Al(111) surface than that for O2 on acetate in Figure 13b. This occurs because there would be more unoccupied e^- states for O3 than for O2 to make the binding energy of VPA adsorption on the Al(111) surface stronger than that of EA adsorption on the same surface.

Figure 14a shows the modified charge DOS for O3 on vinyl phosphonate in Figure 13a, corresponding to unoccupied e^- states (above the E_{lumo}) in Figure 5a. By comparing DOS in Figure 14a to that in Figure 5a for O3 on VPA only, we may

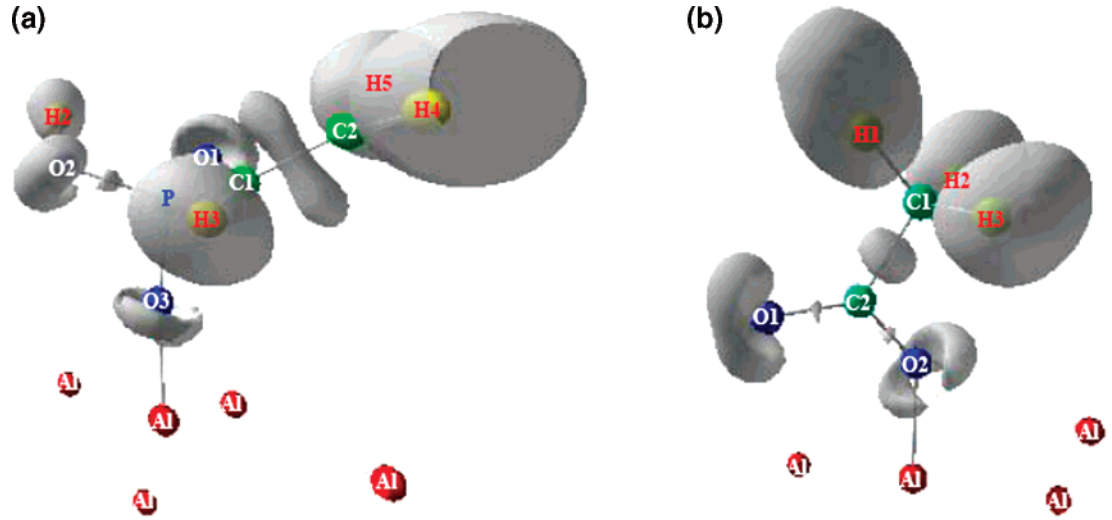

Figure 13. Isosurfaces of charge density at ELF = 0.67 for adsorbates on the Al(111) surface in unidentate coordinations: (a) vinyl phosphonate on the surface and (b) acetate on the surface.

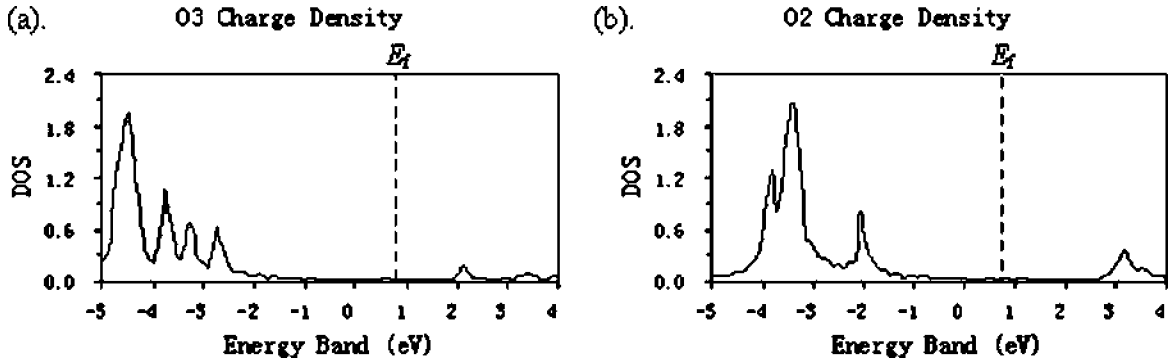

Figure 14. DOS for O ions adsorbed on the surface in unidentate geometry: (a) DOS for O3 on vinyl phosphonate and (b) DOS for O2 on acetate.

find that many of the unoccupied e^- states become occupied (below the E_F, the Fermi level on the energy band) after VPA is adsorbed on the Al(111) surface. Similarly, Figure 14b shows the modified DOS for O2 on acetate in Figure 13b, corresponding to unoccupied e^- states (above the E_{lumo}) in Figure 5b. Comparing O2 on EA to O3 on VPA, we may find that the DOS for O3 shifts more below the E_F than that for O2 after adsorptions, which makes the binding energy of the former adsorption stronger than the latter.

Similar trends of DOS curves in Figure 14 can also be observed for O ions reacting with the Al(111) surface on bi-bridged (VPA and EA) and tribridged (VPA) structures. In all of these cases, the VPA will bind stronger than EA because of the large number of unoccupied e^- states available for bonding to the surface.

2. Corroborations with Experimental Observations. Study of IETS for VPA adsorption on a hydroxylated α-Al_2O_3 slab found that the C═C vibrational frequency on VPA was essentially changed little compared with that before adsorption, which meant that VPA did not react with the surface through its vinyl group which had a C═C bond. Instead, it apparently bonded to the alumina surface through its tripodal "oxygen-rich" base.[29] Similarly, we calculated vibrational frequency of the C1═C2 double bond on a free VPA molecule with the biased Hessian method in VASP[30] and found that $f_{[C1=C2]} = 1718\ cm^{-1}$. The vibrational frequency of such double bond on vinyl phosphonate in tribridged coordination adsorbed on the Al(111) surface was calculated in the same way and was found to be only slightly different; that is, $f_{[C1=C2]} = 1697\ cm^{-1}$. These calculations are consistent with our interpretation: The vinyl tail on VPA does not directly react with the pure aluminum surface.

Similarly, Crowell et al. investigated acetate on the Al(111) surface with EELS. They found that EA was adsorbed on the Al(111) surface through dissociation of the O−H bond at a temperature as low as 120 K.[31] In their "off-specular" observations at 120 K, the most likely binding state of acetate on the Al(111) surface was a symmetrically bi-bridged bonding orientation, which is consistent with our calculations in section 5.2.

6. Further Decomposition Pathways for Acid Molecules on the Al(111) Surface

In this section, two reaction pathways for further decompositions of VPA and EA on the Al(111) surface are discussed. Initially, both of the acid molecules are observed to weakly anchor to the Al(111) surface at S-1 as described in Figure 7. Further decomposition of these molecules on the surface leads to Figure 11 and Figure 12, respectively. For further decompositions, we consider the following steps:

A. Figure 15 shows a side view for further decomposition of EA on the Al(111) surface based on the starting state shown in Figure 11. That is, at step one, one H ion is assumed to dissociate from the O−H bond on EA, and then these two separated pieces are adsorbed on the surface at S-1; the relevant reaction pathway is given by

$$EA + 3Al \rightarrow H_3CC{-}2O...2Al + H...Al, \qquad \Delta H^{(5.7a)}_{ads} = -1.52\ eV \quad (5.7a)$$

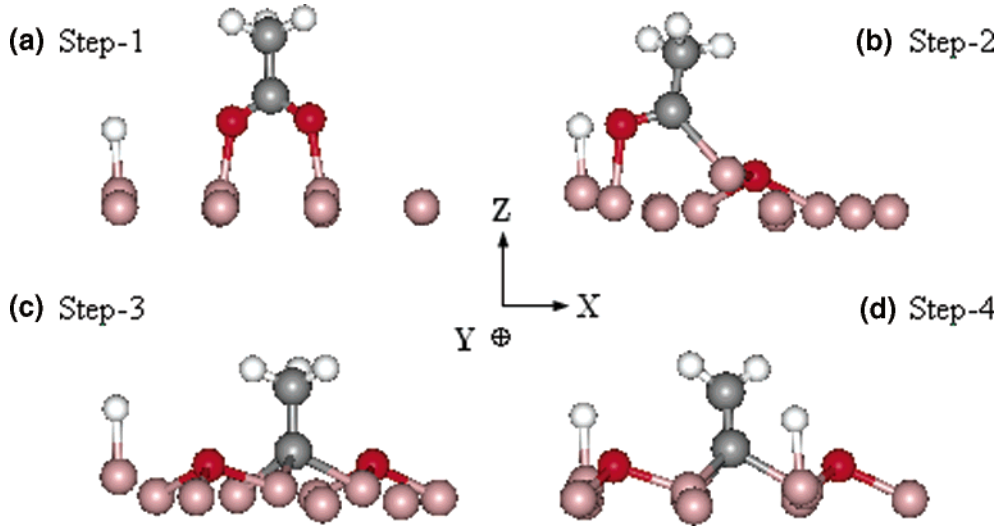

Figure 15. Side view of further decomposition for EA on the Al(111) surface.

At step two, an O ion is assumed to dissociate from H_3CC-2O to anchor to the surface. The C ion at the end of the alkyl chain begins attaching to the surface; the relevant reaction pathway based on eq 5.7a is given by

$$H_3CC-2O...2Al + H...Al \rightarrow H_3C-C(O)...2Al + O...3Al + H...Al, \quad \Delta H^{(6.1)}_{ads} = -1.68 \text{ eV} \quad (6.1)$$

At step three, the second O ion on the main $H_3C-C(O)$ piece undergoes the same behavior as the first O ion to react with surface. The residual alkyl chain completely anchors to the surface in tetracoordination via a C ion at one point; the relevant reaction pathway based on eq 6.1 is given by

$$H_3C-C(O)...2Al + O...3Al + H...Al \rightarrow H_3C-C...3Al + 2(O...3Al) + H...Al, \quad \Delta H^{(6.2)}_{ads} = -1.20 \text{ eV} \quad (6.2)$$

At step four, following the above eq 6.2, one H ion is assumed to dissociate from the residual alkyl chain and is adsorbed on the surface; the relevant reaction pathway is given by

$$H_3C-C...3Al + 2(O...3Al) + H...Al \rightarrow H_2C-C...3Al + 2(O...3Al) + 2(H...Al), \quad \Delta H^{(6.3)}_{ads} = +1.22 \text{ eV} \quad (6.3)$$

Apparently, such a reaction in eq 6.3 is unfavorable to that in eq 6.2.

Comparing all of the above reaction enthalpies (binding energies), we may conclude that the most stable decomposition state is at step three, assuming no other reactions with environment and ignoring entropy effects.

In experimental observations, through using EELS, Crowell et al. found that, when increasing to room temperature, molecular decomposition of EA on the Al(111) surface could continue. Specifically, they found that EA separated into two pieces: (1) The complete liberation of oxygen ions from the original acid molecule oxidized the surface and (2) the residual alkyl chain attached to the surface via a carbon ion at the end of the chain.[31] Therefore, the resultant reaction of EA with the Al(111) surface will lead to oxidization of the surface and formation of acetate on the surface, which corresponds to step three.

B. Figure 16 shows a top view for further decomposition of VPA on the Al(111) surface starting from its tribridged adsorption geometry shown in Figure 12.

In this figure, at step one, two H ions are assumed to dissociate from VPA, and one O ion dissociates from $H_3C_2-PO_3$. Simultaneously, these three ions are adsorbed on the Al-(111) surface: Two H ions are located at two Al ion tops, and an O ion is at one point in the surface, with the residual $H_3C_2-PO_2$ piece anchoring to the surface in bi-bridged coordination via two O ions; the relevant reaction pathway can be given by

$$VPA + 7Al \rightarrow H_3C_2P-(2O)...2Al + 2(H...Al) + O...3Al, \quad \Delta H^{(6.4)}_{ads} = -3.02 \text{ eV} \quad (6.4)$$

At step two, another O ion dissociates from $H_3C_2P(2O)$ and anchors to the surface in the same way as the first liberated O ion did, and then the residual H_3C_2PO anchors to the surface in a tribridged coordination via P and last O ions; the relevant reaction pathway based on eq 6.4 is given by

$$H_3C_2P-(2O)...2Al + 2(H...Al) + O...3Al \rightarrow H_3C_2-P(O)...3Al + 2(H...Al) + 2(O...3Al), \quad \Delta H^{(6.5)}_{ads} = -0.73 \text{ eV} \quad (6.5)$$

At step three, the last O ion also dissociates from the main H_3C_2PO piece and reacts with the surface in the same geometry as the former two O ions assumed. Finally, the residual vinyl group anchors to the surface in tetracoordination via a P ion; the relevant reaction pathway based on eq 6.5 is given by

$$H_3C_2-P(O)...3Al + 2(H...Al) + 2(O...3Al) \rightarrow H_3C_2-P...3Al + 2(H...Al) + 3(O...3Al), \quad \Delta H^{(6.6)}_{ads} = -1.33 \text{ eV} \quad (6.6)$$

At step four, following eq 6.6, one H ion is assumed to dissociate from the residual vinyl group and is adsorbed on the surface. This step is used to examine which of the above configurations can be the most stable. Note that, at step four, the H ion adsorption site on the Al ion top is found to be more stable than that on the O ion. The relevant reaction pathway is given by

$$H_3C_2-P...3Al + 2(H...Al) + 3(O...3Al) \rightarrow H_2C_2-P...3Al + 3(H...Al) + 3(O...3Al), \quad \Delta H^{(6.7)}_{ads} = +1.14 \text{ eV} \quad (6.7)$$

Apparently, the reaction in eq 6.7 is unfavorable to that in eq 6.6.

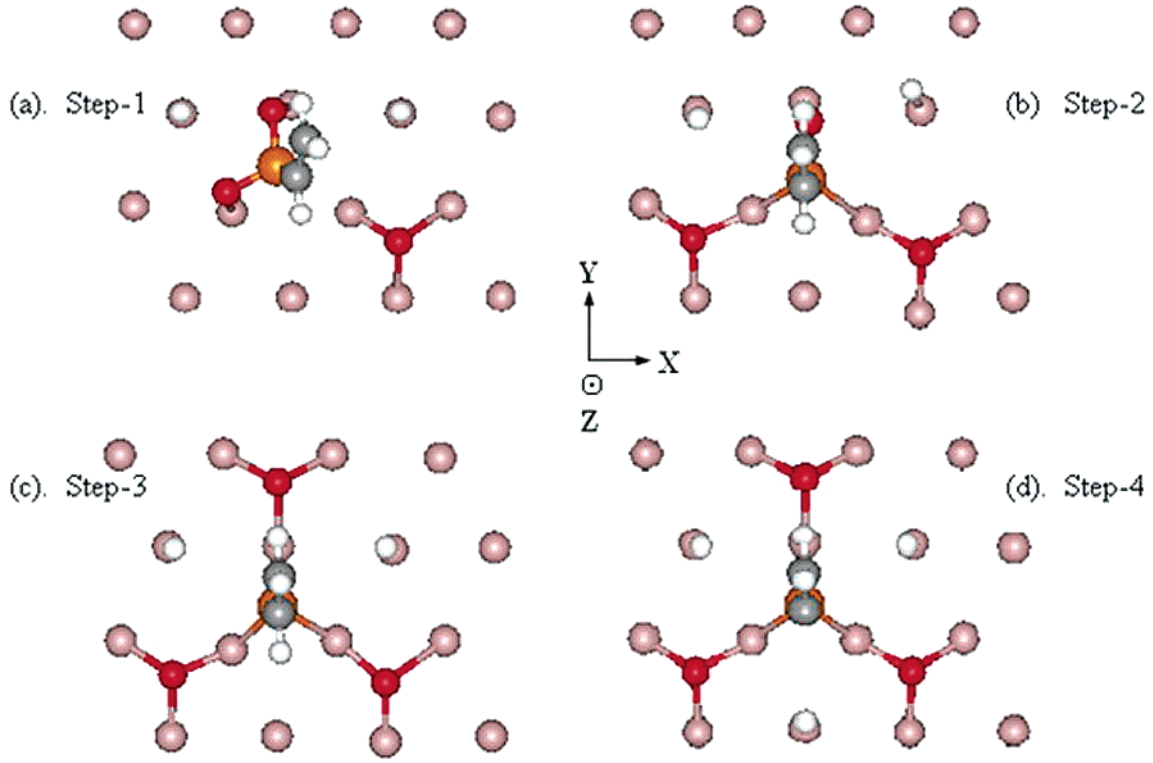

Figure 16. Top view of further decomposition for VPA on the Al(111) surface.

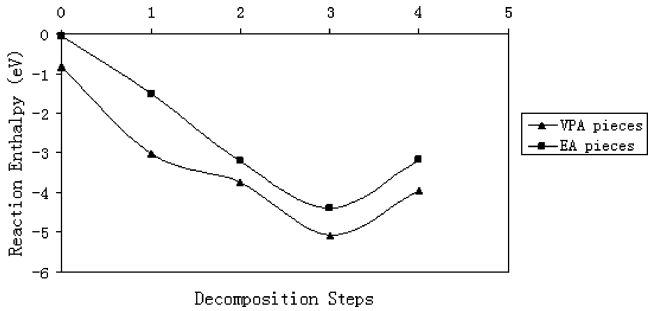

Figure 17. Reaction enthalpies for VPA & EA pieces at relevant decomposition steps.

Our final calculations predict that step three in Figure 16 is the most stable decomposition state among those we investigated. Also at step three, all of dissociated pieces from VPA can be assumed to adhere to the surface, thereby coating it and inhibiting further reaction. Through using the X-ray photoelectron spectroscopy (XPS), Underhill and Timsit observed decomposition pathways of various aliphatic acids (similar to VPA and EA) and alcohols on the Al(111) surface.[5] They found that, at room temperature, the carboxylic (C−O) group on acid molecules decomposed on a clean aluminum surface, resulting in formations of two molecular pieces. One piece was probably deprotonated and bound to the surface with O ions in the OH functional group. The other piece was formed following complete liberation of oxygen from acid molecules and attached itself to a metal surface via a carbon ion originally present in the carboxyl group. This led to attachments of residual alkyl chains to the aluminum surface via a carbon ion at the end of the chain and led to oxidation of the surface. Therefore, our calculations for VPA and EA decompositions are consistent with their experimental observations for similar molecules.[32]

Figure 17 shows curves of reaction enthalpies corresponding to all of the above-mentioned decomposition pathways for acid molecules on the Al(111) surface. From this figure, we may conclude that step three is the most favorable decomposition geometry, assuming no significant entropy contributions.

7. Conclusions

DFT calculations for adsorption and decomposition states of $H_3C_2P(O)(OH)_2$ and $H_3CC(O)(OH)$ on the Al(111) surface were performed for various reaction geometries: tribridged, bi-bridged, and unidentate coordinations. The binding energies for such various adsorption geometries were calculated. The following conclusions can be drawn:

(1) At the initial stage of adsorption, oxygen null groups (oxygen atom linking the pivot P atom with double bonds) on each of the acid molecules allow molecules to weakly anchor to the Al(111) surface.

(2) At the further stage of adsorption with OH group, the most favorable geometry for VPA adsorption on the Al(111) surface was in tribridged coordination, and a bi-bridged coordination was the most favorable for EA adsorption on the Al(111) surface. The adsorption geometry in unidentate coordination on the surface for these two molecules was least favorable. The formation of gaseous H_2 molecules through H atoms desorbed from the Al(111) surface may occur.

(3) The binding energy of VPA adsorption on the Al(111) surface was stronger than that of EA adsorption in similar adsorption geometries. The DOS analyses for O ions on VPA and EA revealed that more unoccupied e^- states for O ions on VPA led to stronger binding energies of VPA than EA during surface adsorptions.

(4) Further acid molecular decompositions on Al(111) led to the attachment of the alkyl chain to the Al(111) surface via carbon or phosphorus ions, plus led to the oxidation of the surface due to complete liberation of oxygen ions from hydroxyl groups on acid molecules. This was consistent with experimental studies using EELS and XPS.

Acknowledgment. This project was sponsored by the National Science Foundation under Grand DMR 9619353.

Computation support was provided through the IBM-p690 on NCSA at The University of Illinois at Urbana−Champaign. The authors would like to thank Dr. Louis G. Hector, Jr., in Materials and Processes Lab at General Motor R & D Center, Michigan, for his very valuable comments on this work. The authors also thank Dr. Yong Jiang in Science and Engineering of Materials Program, Dr. Newton Ooi in Department of Chemical and Materials Engineering, both at Arizona State University, for their pertinent suggestions to this research.

References and Notes

(1) Coast, R.; Pikus, M.; Henriksen, P. N.; Nitowski, G. A. *J. Adhes. Sci. Technol.* **1996**, *2*, 101.
(2) Nitowski, G. A. Ph.D. Dissertation, Virginia Polytechnic State University, 1998.
(3) Ramsier, R. D.; Henriksen, P. N.; Gent, A. N. *Surf. Sci.* **1988**, *203*, 72.
(4) Wefers, K.; Nitowski, G. A.; Wieserman, L. F. U.S. Patent 5,126,-210, 1992.
(5) Underhill, R.; Timsit, R. S. *J. Vac. Sci. Technol., A* **1992**, *10*, 2767.
(6) Chen, J. G.; Crowell, J. E.; Yates, J. T., Jr. *Surf. Sci.* **1986**, *172*, 733.
(7) Lundquist, B. I.; Bogicevic, A.; *Surf. Sci.* **2001**, *493*, 253.
(8) Zhou, H.; Tamura, H.; *Appl. Surf. Sci.* **2000**, *158*, 38.
(9) Jiang, Y.; Adams, J. B. *Surf. Sci.* **2003**, *529*, 428.
(10) Jiang, Y.; Adams, J. B.; Sun, D. *J. Phys. Chem. B* **2004**, *108*, 12851.
(11) Hector, L. G., Jr.; Adams, J. B.; *Surf. Sci.* **2001**, *494*, 1.
(12) Cotton, F. A.; Wilkinson, G. *Advanced Inorganic Chemistry*, 5th ed.; Wiley−Interscience: New York, 1988.
(13) Hohenberg, P.; Kohn, W. *Phys. Rev. A* **1964**, *136*, 864.
(14) Kohn, W.; Sham, L. *Phys. Rev. A* **1965**, *140*, 1113.
(15) Jones, R. O.; Gunnarsson, O. *Rev. Mod. Phys.* **1989**, *61*, 689.
(16) Vanderbilt, D. *Phys. Rev. B* **1990**, *41*, 7892.
(17) Blöchl, P. E. *Phys. Rev. B* **1994**, *50*, 17953.
(18) Perdew, J. P.; Wang, Y. *Phys. Rev. B* **1986**, *33*, 8800.
(19) Perdew, J. P.; Chevary, J. A.; Vosko, S. H.; Jackson, K. A.; Pederson, M. R.; Singh, D. J.; Fiolhais, C. *Phys. Rev. B* **1992**, *46*, 6671.
(20) Murnaghan, F. D. *Proc. Natl. Acad. Sci. U.S.A.* **1944**, *30*, 244.
(21) Ercolessi, F.; Adams, J. B. *Europhys. Lett.* **1994**, *26*, 583.
(22) Monkhorst, H. J.; Pack, J. D. *Phys. Rev. B* **1976**, *13*, 5188.
(23) http://environmentalchemistry.com/yogi/periodic/crystal.html.
(24) Kresse, G.; Furthmüller, J. *VASP the GUIDE*, http://cms.mpi-.univie.ac.at/vasp.
(25) Kresse, G.; Hafner, J. *Phys. Rev. B.* **1993**, *48*, 13115; Kresse, G.; Hafner, J. *Phys. Rev. B.* **1996**, *54*, 11169.
(26) Hernandez-Laguna, A.; Sainz-Diaz, C. I.; Smeyers, Y. G.; de Paz, J. L. G.; Galvez-Ruano, E. *J. Phys. Chem.* **1994**, *98*, 1109.
(27) Derissen, J. L. *J. Mol. Struct.* **1971**, *7*, 67.
(28) Baerends, E. J.; Ellis, D. E.; Ros, P. *Chem. Phys.* **1973**, *2*, 41.
(29) Ramsier, R. D.; Henriksen, P. N.; Gent, A. N. *Surf. Sci.* **1988**, *203*, 72.
(30) Kresse, G.; Furthmüller, J. *Comput. Mater. Sci.* **1996**, *6*, 15.
(31) Crowell, J. E.; Chen, J. G.; Yates, J. T., Jr. *J. Electron Spectrosc. Relat. Phenom.* **1986**, *39*, 97.
(32) Schoofs, G. R.; Benziger, J. B. *Surf. Sci.* **1984**, *143*, 359.
(33) Siegel, D. J.; Hector, L. G., Jr.; Adams, J. B. *Phys. Rev. B* **2002**, *65*, 085415.
(34) http://wulfenite.fandm.edu/Data%20/Table_6.html.
(35) Pauling, L. C. *The Nature of The Chemical Bond*, 3rd ed.; Cornell University Press: New York, 1960.
(36) Touloukian, Y. S.; *Thermophysical Properties of Matter*; Plenum: New York, 1975; Vol. 12.
(37) Simmons, G.; Wang, H. *Single Crystal Elastic Constants and Calculated Aggregate Properties: A handbook*, 2nd ed.; MIT Press: Cambridge, MA, 1971.